MINISTRY OF EDUCATION AND TRAINING

VIETNAM ACADEMY OF SCIENCE AND TECHNOLOGY

GRADUATE UNIVERSITY SCIENCE AND TECHNOLOGY

Nguyen Ngoc Tien

Research on the Synthesis of Composite Materials Based on Metal-Organic Frameworks and Carbon Nanotubes for the Manufacture of Electrochemical Sensors to Analyze Bisphenol A and Paracetamol

SUMMARY OF DISSERTATION ON SCIENCES OF MATTER

Major: Theoretical chemistry and physical chemistry

Code: 9 44 01 19

Ha Noi - 2025

The thesis was completed at: Graduate University Science and Technology - Vietnam Academy of Science and Technology

Supervisors:

Supervisors 1: Dr. Vu Thi Thu - Hanoi University of Science and Technology, Vietnam Academy of Science and Technology

Superivors 2: Assoc. Prof. Dr. Vu Thi Thu Ha - Vietnam Academy of Science and Technology

Referee 1:

Referee 2:

Referee 3:

The dissertation is examined by Examination Board of Graduate University of Science and Technology, Vietnam Academy of Science and Technology at .... /...../2025

The dissertation can be found at:

1. Graduate University of Science and Technology Library

2. National Library of Vietnam

INTRODUCTION

1. Reason for Choosing the Topic

Water pollution with phenolic compounds can lead to serious issues in public health and ecology system. The environment practice agency (EPA) sets the maximum concentration of phenolic compounds in surface water at approximately 1 ppb, and the QCVN stipulates the maximum concentration of total phenolic compounds in surface water at 5-20 ppb. The toxicity of phenolic compounds generally exhibits at concentration range of 9-25 mg/L. The conventional technologies such as spectroscopy and chromatography for detection of phenolic compound are generally time-consuming, require highly skilled technians and expensive instruments. Thus, it is highly demanded to develop novel sensing tools for fast and accurate detection of those compounds. And electrochemical sensors have been demonstrated to be a suitable technical solution for rapid analysis of water pollutants with high reliability and the ability to perform on-site measurements.

To improve the performance of electrochemical sensors, it is critical to choose good electrode material. Metal and/or oxide nanoparticles, conducting polymers, two-dimensional materials (i.e, graphene) have been widely employed to improve the electrochemical signals. In this thesis, the author chooses metal-organic framework (MOF) as electrode materials to improve the sensing performance of electrochemical sensors for detection of phenolic compounds (i.e, bisphenol A, paracetamol). The pore structure made by metal centers and organic ligands is very beneficial to improve the adsorption of aeromatic compounds onto electrode surface. The metal centers might be also involved in catalytic processes to increase the recorded electrochemical signals. The MOF materials will be synthesized using the solvothermal or electrochemical methods. The as-synthesized materials will be used to modify glassy carbon electrodes for analysis of phenolic compound in water.

The topic of the thesis is "Research on the Synthesis of Composite Materials Based on Metal-Organic Frameworks and Carbon Nanotubes for the Manufacture of Electrochemical Sensors to Analyze Bisphenol A and Paracetamol " with the following research objectives and contents:

2. Research Objectives

To synthesize composite materials based on MOF and CNT and then employ them in electrochemical sensors for the rapid and sensitive detection of phenolic compounds in water.

3. Research Contents

- Synthesize a number of new composite materials based on MOF materials containing Zr, Cu, Fe, Ni, and CNT using solvothermal and electrochemical methods.

- Characterize the structure, morphology, and electrochemical properties of the synthesized materials using modern physico-chemical techniques such as X-ray diffraction (XRD), infrared spectroscopy (FT-IR), scanning electron microscopy (SEM), X-ray photoelectron spectroscopy (XPS), energy dispersive X-ray (EDX), nitrogen adsorption-desorption isotherms (BET), thermogravimetric analysis (TGA), etc.

- Apply the as-prepared composite materials to fabricate electrochemical sensors for rapid analysis of bisphenol A (BPA) and paracetamol (PA) in water.

CHAPTER 1. OVERVIEW

The overview section gathers and analyzes both domestic and international research on issues related to the content of this thesis.

1.1. Overview of Phenolic Compounds

1.2. Overview of Metal-Organic Framework (MOF) Materials

1.3. Overview of Carbon Nanotube (CNT) Materials

1.4. Electrochemical Sensors and Their Applications

CHAPTER 2. EXPERIMENTAL METHODS

2.1. Equipment, Instruments, Chemicals

2.2. Methods of Material Synthesis

This section presents the synthesis methods for M-BTC single-metal MOF materials (where M is Cu, Zr, Ni, or Fe), M,M'-BTC two-metal BMOF materials, M,M'-BTC/CNT composite materials (where M, M' are two of Cu, Zr, Ni, or Fe), and the electrochemical synthesis of Cu-BTC films on GCE substrates.

2.2.1. Synthesis of M-BTC Materials (M is Cu, Zr, Ni, or Fe)

The synthesis of Cu-BTC, Zr-BTC, Ni-BTC, and Fe-BTC materials (collectively referred to as M-BTC, where M represents metal ions) is

described in Figure 2.1. The synthesis process for Zr-BTC, Ni-BTC, and Fe-BTC follows a similar procedure to Figure 2.1, with the only difference being the replacement of $CuCl_2.2H_2O$ with the corresponding salts.

Figure 2.1. Synthesis Process of Cu-BTC Material

2.2.2. Synthesis of Two-Metal MOF Materials (M,M'-BTC)

The synthesis process of Zr,Cu-BTC material is shown in Figure 2.2. The Ni,Cu-BTC and Fe,Ni-BTC materials are synthesized using a similar process as shown in Figure 2.2, with the only difference being the substitution of the mixture (1.64 g $CuCl_2.2H_2O$ and 0.77 g $ZrOCl_2.8H_2O$) with the corresponding salt mixtures.

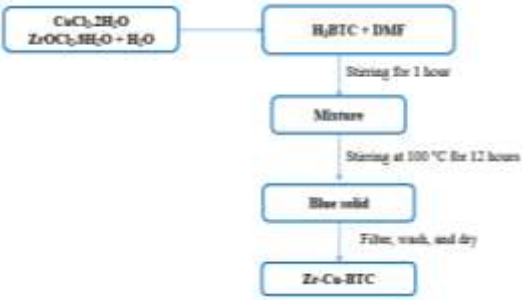

Figure 2.2. Synthesis Process of Zr,Cu-BTC Material

2.2.3. Synthesis of M,M'-BTC/CNT Composite Materials

The synthesis process of the Zr,Cu-BTC/CNT composite material is shown in Figure 2.3. The Ni,Cu-BTC/CNT and Fe,Ni-BTC/CNT materials are synthesized similarly to the process in Figure 2.3, with the only difference being the substitution of the mixture (1.64 g $CuCl_2.2H_2O$, 0.77 g $ZrOCl_2.8H_2O$, and 0.8 g CNT) with the corresponding salt mixtures.

Figure 2.3. Synthesis Process of Cu,Zr-BTC/CNT Composite Material

2.2.4. Electrochemical Synthesis of Cu-BTC Film on GCE Substrate

Cu-BTC is synthesized using the cyclic voltammetry (CV) method. To prepare the solution, 10 ml of DMF is mixed with 13.85 µl of Et3N (Solution 1), followed by the addition of 31.5 mg of H3BTC and 17.1 mg of CuCl2·2H2O to Solution 1 (Solution 2). Solution 2 is then vigorously stirred for 5 minutes using a magnetic stirrer.

The electrode system is assembled, and Solution 2 is poured into the setup to fabricate the Cu-BTC/GCE modified electrode. The electrochemical deposition of the Cu-BTC film is initially investigated using cyclic voltammetry (CV) with a potential range of -1.6 to 0V at a scan rate of 50 mV/s for 10 cycles.

2.3. Methods for Characterizing Materials

2.3.1. Scanning Electron Microscopy (SEM)

Scanning Electron Microscopy (SEM) is used to determine the morphology, shape, particle size, and size distribution of the material. The samples are analyzed using the FE-SEM JEOL JSM-IT800SHL at Hanoi University of Science and Technology.

2.3.2. Energy Dispersive X-ray Spectroscopy (EDX)

The EDX method is used for qualitative and quantitative analysis of elements in the sample. In this study, the materials are analyzed using the HITACHI S-4800 with an accelerating voltage of 10 kV, a resolution from 200 nm to 1 µm, and a working distance (WD) of 7.7 mm. The measurements are performed at the Institute of Materials Science, Vietnam Academy of Science and Technology.

2.3.3. X-ray Diffraction (XRD)

XRD is used to identify the phase structure, phase composition, space group, lattice size, and purity of the material. In this study, XRD patterns are

recorded using the AXS D8-Advance, Brucker with CuKα radiation at 40 kV and 15 mA current, with a wavelength λ = 1.5406 Å. The XRD measurements are carried out at Hanoi University of Science and Technology.

2.3.4. Fourier Transform Infrared Spectroscopy (FT-IR)

FT-IR is used to identify the chemical bonds and functional groups in the material sample. In this study, the materials are analyzed using the Thermo Electron Scientific Nicolet iS50 FT-IR system at Hanoi University of Science and Technology.

2.3.5. Nitrogen Adsorption-Desorption Isotherms (BET)

This method is used to determine the specific surface area (m^2/g), total pore volume (cm^3/g), average pore diameter (nm), and pore size distribution of the material. In this study, the samples are analyzed on a Tristar-3030 system (Micromeritics-USA) at 77K using liquid nitrogen as the coolant, at the Institute of Chemistry, Vietnam Academy of Science and Technology.

2.3.6. X-ray Photoelectron Spectroscopy (XPS)

XPS is used to determine the binding energy of electrons in the sample. The binding energy is characteristic of the atoms and provides essential information about the elements present in the sample, their percentage content, and their oxidation states. In this thesis, the XPS spectra are measured using the THERMO VG SCIENTIFIC MultiLab2000 (UK) system.

2.3.7. Raman Spectroscopy

Raman Spectroscopy is used to identify characteristic vibrational modes of atoms in the sample and to study the molecular vibration mechanisms, atomic group vibrations in materials, or the simultaneous vibrations of the crystal lattice. In this thesis, Raman spectra are recorded using the Horiba LabRAM HR Evolution system with a resolution of 0.5 cm^{-1}/pixel at a wavelength of 532 nm.

2.3.8. Thermogravimetric Analysis (TGA)

TGA is used to investigate the weight change of the material sample as the temperature is increased from room temperature to 800°C. In this study, TGA measurements are performed using the Linseis TGA PT 1600 system with a temperature range from room temperature to 800°C and a heating rate of 10°C/min at Hanoi University of Industry.

2.4. Electrode Modification Methods

2.4.1. GCE electrode preparation

2.4.2. GCE Electrode Modification by Drop Casting

This method involves creating a thin film by dissolving/dispensing the modified material in a solution and directly dropping it onto the working electrode surface. The material is dispersed in ethanol to form a 1.0 mg/mL solution, which is then sonicated for about 1 hour. A 5 µL aliquot of this solution is dropped onto the GCE electrode to completely cover the electrode surface. The solvent is allowed to evaporate at room temperature for 60 minutes, and the electrode surface is then lightly dried at 60°C for 30 minutes.

2.4.3. GCE Electrode Modification by Electrochemical Method

This technique involves sweeping the potential to form polymerized products of the modified material on the GCE surface or using potential application to precipitate the material on the electrode surface. The electrochemical synthesis method allows the material to be deposited on the electrode surface, with the process controlled precisely by synthesis time, applied potential, and current intensity.

2.5. Electrochemical Methods for Evaluating Sensor Performance

2.5.1. Cyclic Voltammetry (CV)

2.5.2. Differential Pulse Voltammetry (DPV)

2.5.3. Sensor Performance Optimization

BPA detection in water is carried out using the Differential Pulse Voltammetry (DPV) method in the range of 300 to 800 mV, with a potential step of 5 mV. Experiments are conducted with a 50 µM BPA solution.

2.5.4. Evaluation of Sensor Performance Parameters

2.5.4.1. Evaluation of Electrochemical Signals on the Sensor

After modifying the electrode with different materials at a concentration of 1 mg/mL, measurements are taken in a PBS buffer solution containing BPA at the same concentration under similar operating conditions to compare the electrochemical signals recorded on the modified electrodes. This serves as a basis for evaluating the sensor's performance.

2.5.4.2. Evaluation of Sensor Repeatability and Stability

The repeatability of the sensor is determined by preparing identical electrodes and measuring them in a 5 µM BPA solution using the DPV

method. The stability of the sensor is assessed by preparing 15 identical electrodes, using 2-3 electrodes to measure BPA under the same conditions as the repeatability test. The remaining electrodes are kept for further measurements over the following days. The results from the subsequent measurements are used to determine the stability of the electrode.

CHAPTER III: RESULTS AND DISCUSSION

3.1. Results of Synthesis and Application of Cu,Zr-BTC/CNT Material System

3.1.1. Morphological Characteristics of the Material

The SEM images of the material are shown in Figure 3.1. The Cu-BTC sample exhibits a polyhedral morphology with edge lengths ranging from 5 to 15 µm. The polyhedral structure of the sample is maintained even after the addition of Zr (Cu:Zr = 8:1). From the SEM images, it can be observed that the Cu,Zr-BTC/CNT composite material has a fairly uniform distribution on the surface of the CNT support.

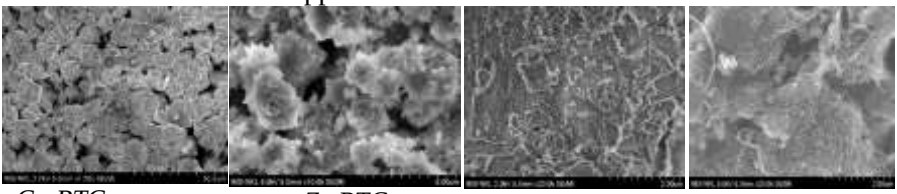

Cu-BTC *Zr-BTC* *Zr,Cu-BTC* *Cu,Zr- BTC/CNT*

Figure 3.1. SEM Images of the Materials

3.1.2. Structural Characteristics and Chemical Composition of the Material

The EDX spectra of the samples were analyzed to determine the elemental composition. The details of the atomic percentages of the elements are presented in Table 3.1.

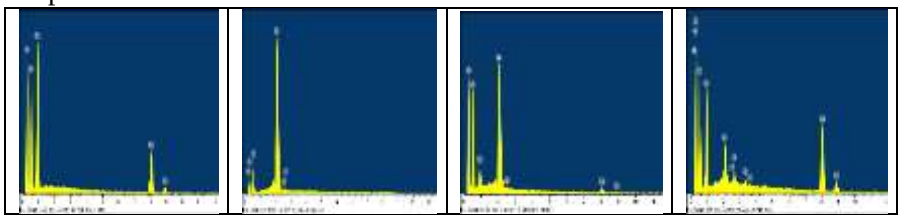

Figure 3.2. EDX Spectra of Cu-BTC(a), Zr-BTC(b), Zr,Cu-BTC(c), and Cu,Zr-BTC/CNT(d)

Table 3.1. Elemental Composition of the Material Samples

Material	Mass composition of elements (%)					Molar Ratio Cu/Zr
	C (%)	O (%)	O/C	Cu (%)	Zr (%)	
Cu-BTC	56.7	39.1	0.69	4.2	-	-
Zr-BTC	51.9	37.4	0.72	-	10.3	-
Cu,Zr-BTC	60.98	33.52	0.55	4.64	0.87	5.33
Cu,Zr-BTC/CNT	63.81	31.27	0.49	4.41	0.52	8.48

The bonding states of the elements in the sample were analyzed from the XPS spectra, as shown in Figure 3.4.

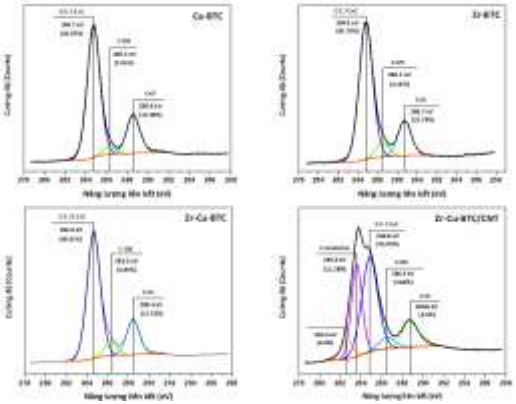

Figure 3.4. XPS C1s Spectra of the Material Samples

The C1s spectra of the Cu-BTC, Zr-BTC, and Cu,Zr-BTC samples show three peaks at binding energies of C=C/C–C (284.7 eV), C–OH (286.3 eV), and C=O (288.6 eV). The XPS C1s spectrum of the Cu,Zr-BTC/CNT sample also reveals two additional peaks at binding energies of 283.6 eV and 282.6 eV, characteristic of CNT vibrations. These results confirm the formation of the composite/MOF material based on the bonding of Cu,Zr-BTC with the CNT support.

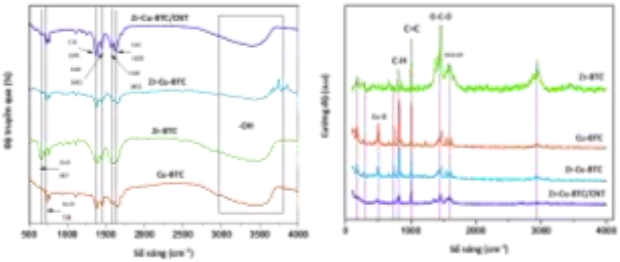

Figure 3.9. FTIR and Raman Spectra of the Material

The FTIR spectra of the samples (Figure 3.9) show asymmetric and symmetric vibrations of the bonds in the carboxylate group of the BTC ligand at 1622 cm^{-1}, 1566 cm^{-1}, 1451 cm^{-1}, and 1371 cm^{-1}. The peaks in the Raman spectra are attributed to the vibrations of C=C and C-H bonds in the BTC ligand, C=C in the benzene ring (1618 and 1006 cm^{-1}), C-H bonds (826 cm^{-1} and 745 cm^{-1}), C-O_2 asymmetric (1552 cm^{-1}) and symmetric (1465 cm^{-1}) vibrations. The peak at 501 cm^{-1} is assigned to Cu-O bonding modes.

3.1.3. Nitrogen Adsorption/Desorption Isotherms of the Materials

The Cu-BTC, Zr-BTC, and Zr,Cu-BTC samples all exhibit Type I adsorption-desorption isotherms with H4 hysteresis loops. In contrast, the Cu,Zr-BTC/CNT samples display Type IV isotherms, with a large hysteresis loop indicating materials with intermediate pore sizes.

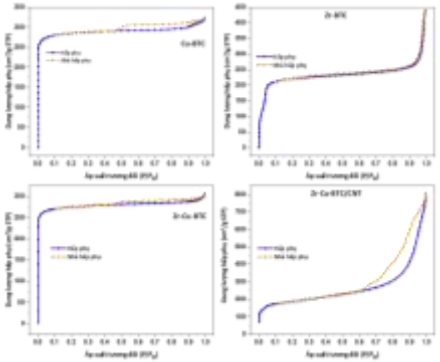

Figure 3.10. Nitrogen Adsorption-Desorption Isotherms of the Samples

3.1.4. TG-DTA Thermal Analysis of the Material

The TG-DTA curves of the materials are shown in Figure 3.11. The TGA curve of all the samples shows five stages of mass loss.

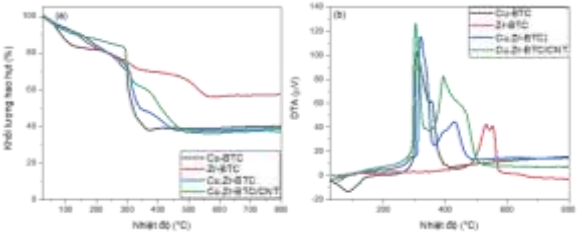

Figure 3.13. TGA Curves of Cu-BTC, Zr-BTC, Cu,Zr-BTC, and Cu,Zr-BTC/CNT Materials

3.1.5. Electrochemical Properties of Cu,Zr-BTC/CNT Material

The electrochemical properties were evaluated in an $[Fe(CN)_6]^{3-}$ solution using Electrochemical Impedance Spectroscopy (EIS). The high conductivity of the CNT material can enhance the electron transfer kinetics on the electrode surface.

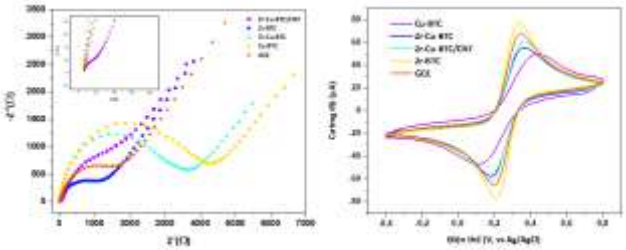

Figure 3.14. EIS and CV Diagrams of Cu-BTC, Zr-BTC, Cu,Zr-BTC, and Cu,Zr-BTC/CNT Materials

3.1.6. Factors Affecting the Electrode Performance

3.1.6.1 Effect of pH

The results show that the current increases as the pH rises from 5 to 8 and decreases at higher pH levels. Therefore, a pH of 8.0 is selected as the optimal value for subsequent experiments.

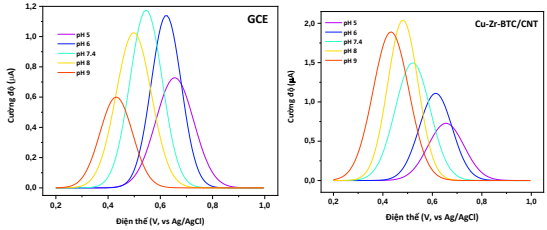

Figure 3.15. Effect of pH on the BPA Oxidation Process at the Electrode

3.1.6.2. Effect of BPA Adsorption Time on the Electrode Surface

The results show that the optimal enrichment time was found to be 180 seconds for the GCE electrode.

3.1.6.3. Effect of Scan Rate

The electrochemical oxidation kinetics of BPA on the Cu,Zr-BTC/CNT modified GCE were studied in PBS containing 10 µM BPA at different scan rates ranging from 10 to 200 mV/s (Figure 3.15). The oxidation peak currents appeared at 550 mV and increased linearly with increasing scan rate as follows: Ipa (µA) = 0.0159v (mV/s) + 0.424 (R2 = 0.9970), indicating an adsorption-

controlled process. Similar kinetics were obtained on the bare GCE with the following linear equation: Ipa (μA) = 0.0104v (mV/s) + 0.4925 (R2 = 0.9934).

3.1.7. Electrochemical Signal of BPA on Modified Electrodes

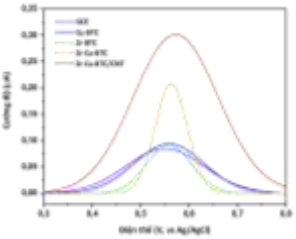

Figure 3.18. DPV Curves Recorded on Different Electrodes in 0.1M PBS Solution Containing 2μM BPA

Schematic of the Reaction Mechanism on the Electrode Surface.

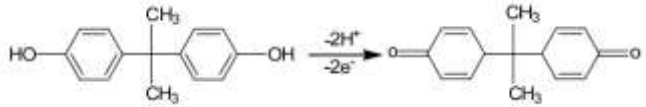

3.1.8. Calibration Curve and Determination of Electrode Performance Parameters

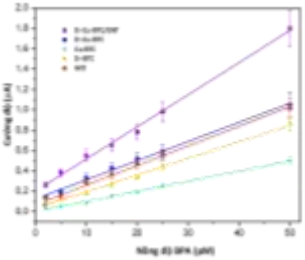

Figure 3.19. Calibration curve

The regression equation is: I (μA) = 0.0316 * CBPA (μM) + 0.2021 (R^2 = 0.9965). The detection limit is 0.50 μM and the sensitivity is 0.451 $\mu A \cdot \mu M^{-1} \cdot cm^{-2}$.

3.1.10. Results of the control sample analysis

Table 3.8. Comparison of BPA measurement results between electrochemical method and HPLC method.

Concentration (ppm)	Method			
	Eectrochemical		HPLC	
	Measured results (ppm)	Recovery (%)	Measured results (ppm)	Recovery (%)
5	4.58	91.60	4.60	92.16
10	9.21	92.11	11.04	110.43
15	14.23	94.91	14.03	93.54

3.2. Results of the synthesis and application of the Fe,Ni-BTC/CNT material system

3.2.1. Morphological characteristics of the material

The SEM measurements of Fe,Ni-BTC/CNT show the simultaneous presence of Fe,Ni-BTC material on the CNT fibers. The size of the CNT is approximately 20 nm, while that of Fe,Ni-BTC is around 2 µm.

3.2.2. Structural characteristics and chemical composition of the material

From the EDX spectrum of Fe,Ni-BTC (Figure 3.21), the presence of Fe, Ni, C, O, and a few other elements from salts like Cl can be observed. Table 3.9 shows the elemental composition of the Fe,Ni-BTC/CNT sample obtained via EDX analysis, confirming the presence and proportion of Ni, Fe, C, O elements in the material.

The FTIR spectrum measurements of Fe,Ni-BTC are presented in Figure 3.22.

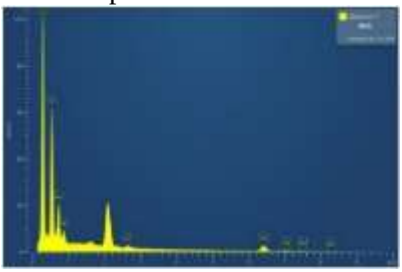

Figure 3.21. EDX spectrum of Fe,Ni-BTC

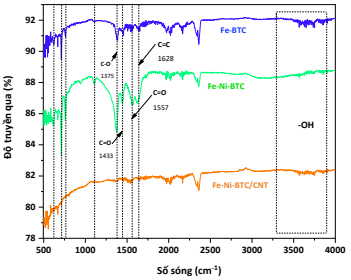

Figure 3.22. FTIR spectrum of Fe,Ni-BTC/CNT

Table 3.9. Elemental composition in Fe,Ni-BTC/CNT

STT	Element	Mass %	Percentage ratio
1	C	71.41	81.66
2	O	18.39	15.79
3	Si	0.37	0.18
4	Fe	6.71	1.65
5	Ni	2.66	0.62

3.2.3. Electrochemical Characteristics of Fe,Ni-BTC/CNT Material

The charge transfer resistance recorded from the electrochemical impedance spectroscopy (EIS) is presented. The charge transfer resistance (Rct) value for the Fe,Ni-BTC/CNT/GCE electrode is 2245.6 Ω, while the Rct for the GCE is 1393.6 Ω. Thus, the charge transfer resistance of the Fe,Ni-BTC/CNT/GCE is significantly higher compared to the GCE.

3.2.4. Factors Affecting the Modified Electrode

3.2.4.1. Effect of pH

The optimal pH value for BPA detection using the Fe,Ni-BTC/CNT/GCE electrode is approximately pH = 7.4.

3.2.4.2. Effect of BPA Adsorption Time on the Electrodes

The results indicate that when the BPA adsorption time on the electrode is 120 seconds, the reactions on the electrode surface occur most stably.

3.2.4.3. Effect of Scan Rate

The survey results show that the scan rate also affects the electrochemical processes on the electrode.

3.2.5. Calibration Curve and Determination of Electrode Performance Parameters

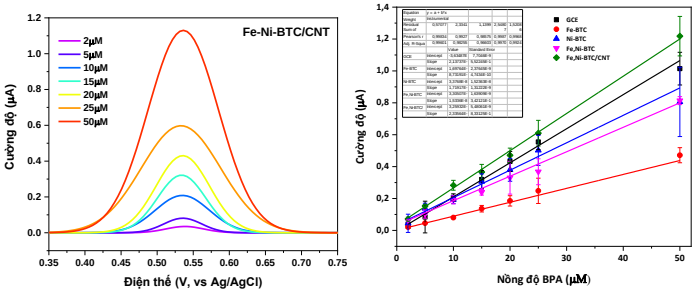

Hình 3. 29. Calibration curve I-C of the modified electrodes and GCE

The equation: I (μA) = 0.0236CBPA + 0.0242 (R2 = 0.9982) and I (μA) = 0.0206CBPA + 0.0042 (R2 = 0.9963) for the two electrodes. The detection limit of Fe,Ni-BTC/CNT/GCE is 0.7 μM, with a sensitivity of 0.334 $\mu A.\mu M^{-1}.cm^{-2}$, and for GCE, the detection limit is 0.82 μM, with a sensitivity of 0.294 $\mu A.\mu M^{-1}.cm^{-2}$.

3.2.6. Results of control sample analysis.

Table 3.15. Comparison of BPA measurement results between electrochemical method and HPLC method

Concentration (ppm)	Method			
	Fe,Ni-BTC/CNT/GCE Electrochemical Sensor		HPLC	
	Measured Results (ppm)	Recovery (%)	Measured Results (ppm)	Recovery (%)
5,00	4.08	81.60	4.42	88.40
10,00	10.14	101.40	9.28	92.80
15,00	14.19	94.60	15.37	102.47

3.3. Synthesis Results and Applications of the Cu,Ni-BTC/CNT Material System

3.3.1. Morphological Characteristics of the Material

The SEM results show that the Cu-BTC material has a cubic bipyramidal shape with a size of about 2 µm, and the crystals are quite porous. The Ni-BTC crystals are cubic with a size ranging from 2-5 µm. Meanwhile, the size and shape of Cu,Ni-BTC depend on the Cu/Ni ratio. The SEM images of the Cu,Ni-BTC material show the simultaneous presence of Cu-BTC and Ni-BTC.

3.3.2. Structural and Chemical Composition Characteristics of the Material

The wide band in the range from 2700 to 3700 cm-1 corresponds to the oscillations of the O-H bond from the water molecules absorbed in the pores of the MOF. The presence of organic ligands and coordination bonds with metals can also be observed in the FTIR spectrum. In addition, the FTIR spectrum shows characteristic bands of the organic ligands and metals.

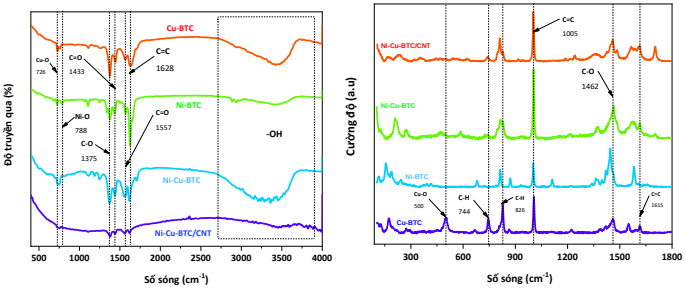

Figure 3.32. FTIR and Raman spectra of Cu-BTC, Ni-BTC, Cu,Ni-BTC, Cu,Ni-BTC/CNT

The Raman spectra display structural features related to the organic ligand, with the main peaks in the Raman spectrum assigned to the vibrations of C=C and C–H in the BTC ligand: C=C in the benzene rings (1005 cm−1); C–H vibration (826 cm−1), C-O2 (1462 cm−1). The band at 500 cm−1 is attributed to the Cu-O bond.

The XPS spectrum shows the presence of the expected elements (C, O, Cu, Ni), as well as the elemental composition presented in Table 3.16.

Table 3.16. Mass composition of elements in the sample

	Element	Materials			
		Cu,Ni-BTC/CNT	Cu,Ni-BTC	Cu-BTC	Ni-BTC
Elemental mass composition (%)	C	89.33	60.84	57.25	60.00
	O	9.12	31.96	34.88	31.4
	Cu	1.38	5.51	6.63	N/A
	Ni	0.17	1.69	N/A	4.31
	N		0	1.24	3.8
Total		100	100	100	100

3.3.3. Factors Affecting the Performance of the Modified Electrode

3.3.3.1. Effect of pH

For the Cu,Ni-BTC/CNT/GCE electrode, the GCE shows the best signal intensity at pH = 7.4.

3.3.3.2. Effect of BPA Adsorption Time on the Electrode

The survey results show that the optimal adsorption time for Cu,Ni-BTC/CNT/GCE is 120 seconds, and for GCE it is 180 seconds.

3.3.3.3. Effect of Scan Rate

The peak oxidation current increases linearly with the scan rate as follows: Ipa (μA) = 0.0098 × v (mV/s) + 0.1123 (R^2 = 0.9904). This indicates a process that is controlled by adsorption. Similar kinetics were also observed on bare GCE, with the following equation: Ipa (μA) = 0.0009 × v (mV/s) + 0.0297 (R^2 = 0.9898).

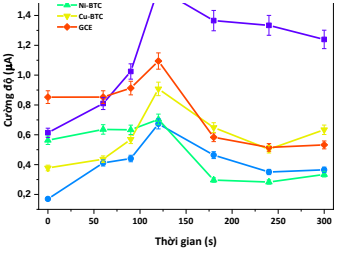

Figure 3.36. Effect of BPA adsorption time on the electrode surface

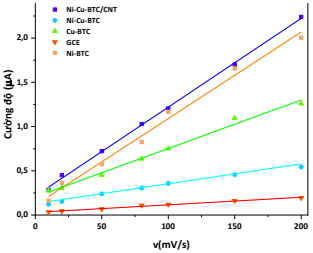

Figure 3.37. Effect of scan rate

3.3.4. Electrochemical Signal of BPA on Cu,Ni-BTC/CNT/GCE Electrode

The electrochemical signals of the modified electrodes were measured in 5 µM BPA at pH 7.4, with a 120s accumulation time. The results showed that the reaction on the Cu,Ni-BTC/GCE electrode was 1.4 to 1.7 times greater than on the other electrodes.

Table 3.17. Electrochemical Signal of 5 µM BPA on Modified Electrodes

STT	Material	Signal (µA)
1	Cu-BTC	0,1214
2	Ni-BTC	0,0978
3	Cu,Ni-BTC	0,107
4	Cu,Ni-BTC/CNT	0,171

3.3.5. Standard curve and determination of the operating parameters of the electrode

The regression equation is as follows:

I (µA) = 0.0337 × CBPA (µM) - 0.0140 (R^2 = 0.9945) with a detection limit of 0.5 µM and sensitivity of 0.481 µA μM^{-1} cm^{-2} for the Cu,Ni-BTC/CNT/GCE electrode.

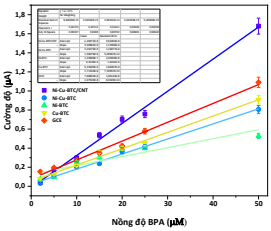

Figure 3.38. Standard curve of BPA on modified electrodes and GCE

Table 3.18. Comparison of the standard curves of modified material sensors

STT	*material*	Standard curve	LOD (µM)	Sensitivity ($\mu A.\mu M^{-1}.cm^{-2}$)
1	Ni,Cu-BTC	I = 0.0158C + 0.0220 R^2 = 0.9948	0.57	0.226
2	GCE	I = 0.0193C + 0.0663 R^2 = 0.9957	0.84	0.283
3	Cu-BTC	I = 0.0171C + 0.0519 R^2 = 0.9913	0.87	0.141
4	Ni-BTC	I = 0.0157C + 0.0534 R^2 = 0.9833	1.07	0.224
5	Cu,Ni-BTC/CNT	I = 0.0337C – 0.0140 R^2 = 0.9945	0.5	0.481

The comparison results of the BPA sensor performance between the Cu,Ni-BTC/CNT/GCE electrode and the Cu,Ni-BTC/GCE electrode show

that the use of CNT, which has high conductivity, improved the sensitivity of the BPA sensor by a factor of 2.1.

3.3.7. Results of the analysis of the control sample

Table 3.21. Comparison of BPA measurement results between the electrochemical method and HPLC

Nồng độ (ppm)	Phương pháp			
	Cảm biến điện hóa Cu,Ni-BTC/CNT/GCE		HPLC	
	Kết quả đo được (ppm)	Độ thu hồi (%)	Kết quả đo được (ppm)	Độ thu hồi (%)
5	4.24	84.80	4.49	89.80
10	9.77	97.70	10.38	103.80
15	13.86	92.40	14.99	99.91

3.4. Electrochemical synthesis results of Cu-BTC film on GCE electrode and its application in the analysis of acetaminophen

3.4.1. Mechanism of Cu-BTC formation process on the electrode surface

The formation of the Cu-BTC film begins with the deprotonation process, which generates BTC^{3-} ions from the organic ligand H_3BTC. The BTC^{3-} then pairs with Cu^{2+} to form Cu-BTC. The crystallization rate of the material on the electrode surface creates a porous, rough film, enhancing the adsorption capacity of the analyte on the surface and ensuring good conductivity of the film.

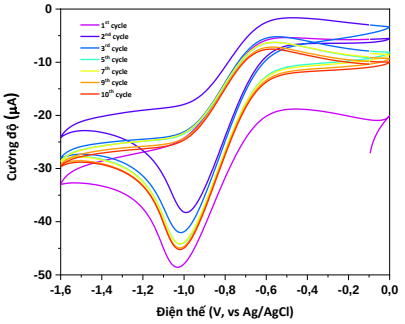

Figure 3.39. CV curve of Cu-BTC synthesis

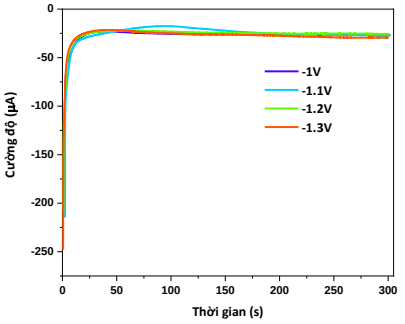

Figure 3.41. CA curve of Cu-BTC synthesis at different applied potentials

The electrochemical synthesis mechanism of Cu-BTC is described in three stages:

- Stage 1: Protonation of triethylamine and reduction of triethylammonium ion:

$$Et_3N + H_2O \longleftrightarrow Et_3NH^+ + OH^-$$

$$2Et_3NH^+ + 2e^- \longrightarrow H_2 + 2Et_3N$$

- Stage 2: Deprotonation of trimesic acid (H_3BTC):

$$H_3BTC + 2e^- \longrightarrow HBTC^{2-} + H_2$$

$$HBTC^{2-} \longrightarrow H^+ + BTC^{3-}$$

- Stage 3: Cu-BTC formation via the pairing of Cu^{2+} ions from $CuCl_2 \cdot 2H_2O$ and BTC^{3-} ions formed in stage 2:

$$3Cu^{2+} + 2BTC^{3-} \longrightarrow Cu_3(BTC)_2$$

Additionally, water from $CuCl_2 \cdot 2H_2O$ is also electrolyzed in parallel with the protonation of Et_3N, which helps accelerate the formation of BTC^{3-} ions by increasing the pH of the solution through the following reaction:

$$2H_2O + 2e^- \longrightarrow H_2 + 2OH^-$$

3.4.2. Structural and Morphological Characteristics of Electrochemically Synthesized Cu-BTC

The SEM image of Cu-BTC on the GCE substrate shows a dense octahedral crystal film of Cu-BTC with a size under 1 μm. The size of the MOF crystals synthesized by the electrochemical method is approximately 10 times smaller than that of the MOF crystals synthesized by the chemical method.

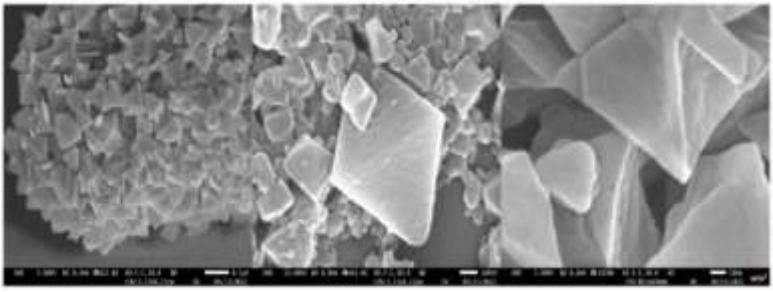

Figure 3.42. SEM image of Cu-BTC on GCE

The functional groups of Cu-BTC were evaluated through FT-IR spectroscopy

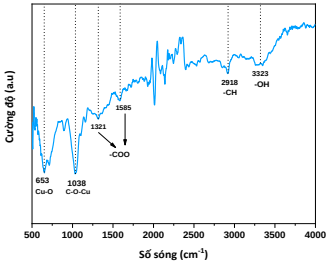

Figure 3.43. FTIR spectrum of Cu-BTC

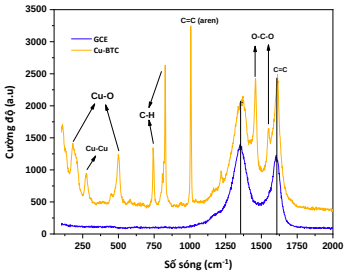

Hình 3.44. Phổ Raman của GCE và Cu-BTC trên điện cực GCE

In the Raman spectrum, the peaks in the range from 100 to 500 cm^{-1} correspond to vibrations related to Cu^{2+} ions. The bending vibrations of the C-H bonds are observed at peaks at 742 cm^{-1} and 827 cm^{-1}, respectively. The peak around 1006 cm^{-1} is the symmetric vibration of the C=C bonds in the benzene ring.

3.4.3. Electrochemical Properties of Cu-BTC Film

3.4.3.1. Investigation with 100 mM KCl Solution

The electrochemical properties of the Cu-BTC film were investigated in a 100 mM KCl electrolyte solution.

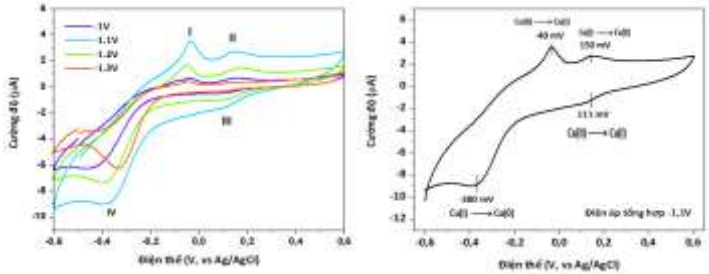

Figure 3.48. CV curve of Cu-BTC/GCE electrode in 100 mM KCl

The Cu-BTC material film synthesized at -1.1 V shows a higher oxidation-reduction peak current intensity compared to films synthesized at other potentials.

3.4.3.2. Electron Transfer Rate Constant and Electron Transfer Resistance

The study evaluated the electron transfer rate on the electrode surface using

the CV method with a 5 mM $[Fe(CN)_6]^{3-/4-}$ solution. Both the anodic current (Ipa) and cathodic current (Ipc), corresponding to the oxidation and reduction peaks for the $[Fe(CN)_6]^{3-} + 1e \leftrightarrow [Fe(CN)_6]^{4-}$ process, increased 1.4 times compared to the bare GCE.

The electrochemical impedance spectroscopy (EIS) results show that the charge transfer resistance (Rct) of the GCE is 2172.5 Ω, while for Cu-BTC/GCE, it is 86 Ω, indicating a 25-fold increase in the conductivity of the electrode.

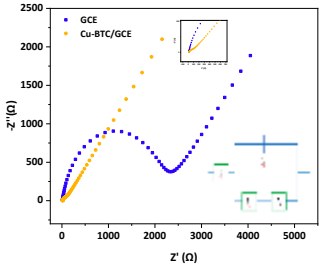

Figure 3.51. Nyquist plot of GCE electrode and Cu-BTC/GCE

3.4.4. Factors Affecting the Oxidation-Reduction Reaction of PA on Modified Electrodes

3.4.4.1. Effect of Scan Rate

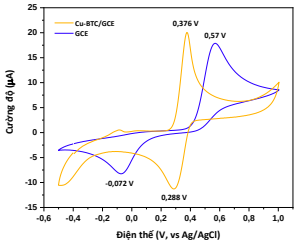

Figure 3.52. CV curve of Cu-BTC/GCE and GCE electrodes in a solution containing 1 mM PA in PBS (pH 7.4)

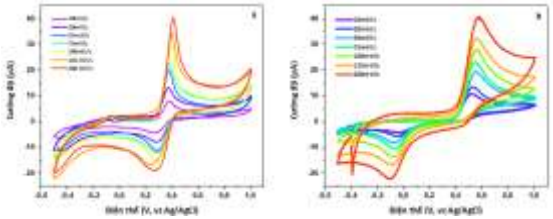

Figure 3.53. CV curve of Cu-BTC/GCE electrode (a) and GCE electrode (b) in 1 mM PA solution at varying scan rates

The kinetics of the electrochemical oxidation process of PA on the modified Cu-BTC/GCE electrode were studied in a PBS solution (pH = 7.4) containing 1 mM PA, with scan rates increasing from 10 to 200 mV/s (Figure 3.51).

The oxidation peak currents appeared at 350 mV, and the intensities of Ipa and Ipc increased linearly with the square root of the scan rate (Figure 3.52), indicating that the process is diffusion-controlled.

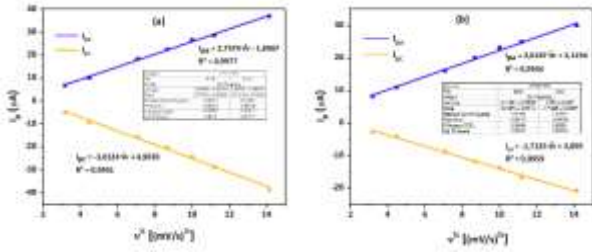

Figure 3.54. Ip vs. $v^{1/2}$ plot for Cu-BTC/GCE electrode (a) and GCE electrode (b)

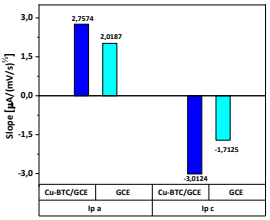

Figure 3.55. Slope of Ipa vs. $v^{1/2}$ and Ipc vs. $v^{1/2}$ for the two electrodes

A similar kinetics were observed with the GCE. On the other hand, the slope of the kinetic calibration curves Ipa vs. $v^{1/2}$ and Ipc vs. $v^{1/2}$ for Cu-BTC/GCE is higher than that of GCE, demonstrating that the presence of Cu-BTC enhances the oxidation reaction rate of PA and increases the detection signal in the solution.

3.4.4.2. Effect of pH

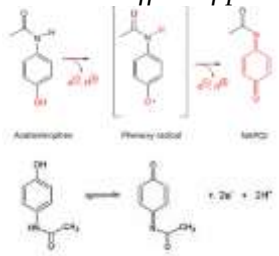

Figure 3.56. Schematic of the oxidation mechanism of PA

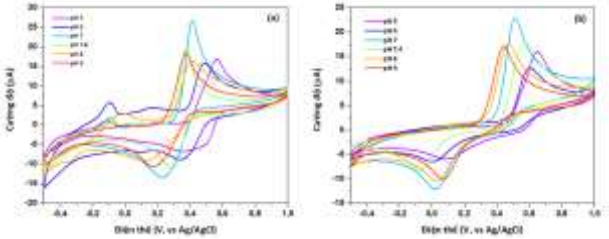

Figure 3.57. CV curve investigating the effect of pH (5 - 9) in 1 mM PA solution for Cu-BTC/GCE electrode (a) and GCE electrode (b)

The mechanism of the oxidation process involves the transfer of two electrons and two protons (H^+) to form the unstable product N-acetyl-p-benzoquinone imine (NAPQI). Therefore, pH is an important parameter affecting the electrochemical oxidation of PA on the electrode surface.

3.4.5. PA Analysis on Modified Electrode

The PA analysis was performed using the square wave voltammetry (SWV) technique. The Cu-BTC/GCE electrode was synthesized by applying a potential of -1.1 V for 5 minutes. The concentration range of PA chosen was from 10 µM to 50 µM.

The results shown in Figure 3.60 indicate that the presence of Cu-BTC on the GCE electrode reduced the oxidation potential of PA from 450 mV to 350 mV. The appearance of Cu-BTC on the electrode surface enhances the charge transfer on the electrode, leading to a faster oxidation reaction of PA.

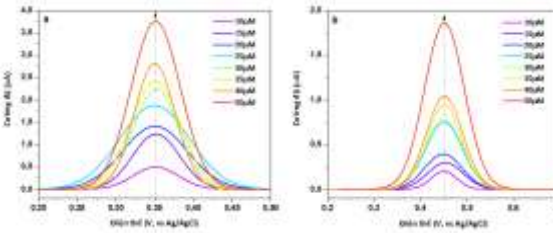

Figure 3.59. SWV curve at different PA concentrations for Cu-BTC/GCE electrode (a) and GCE electrode (b)

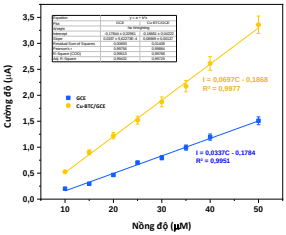

Figure 3.60. Calibration curve of I - C for PA

The calibration curve for Cu-BTC/GCE shows that the peak current intensity increases linearly with the PA concentration from 10-50 µM, following the regression equation: I (µA) = 0.0697 × CPA (µM) – 0.1868 (R^2 = 0.9977). A similar result was observed on GCE: I (µA) = 0.0337 × CPA (µM) – 0.1784 (R^2 = 0.9951). The sensitivity and detection limit for Cu-BTC/GCE are 0.996 $\mu A \cdot \mu M^{-1} \cdot cm^{-2}$ and 0.077 µM, respectively. These results are better than those for the bare GCE electrode (0.481 $\mu A \cdot \mu M^{-1} \cdot cm^{-2}$; 0.203 µM).

CONCLUSION AND PERSPECTIVES

I. Conclusion:

1. Three composite/MOF material systems were successfully synthesized, including: Cu,Zr-BTC/CNT; Fe,Ni-BTC/CNT; Cu,Ni-BTC/CNT, and the characteristic parameters such as morphology, structure, and composition of the materials were evaluated using modern physico-chemical analysis methods.

2. These materials were applied to develop electrochemical sensors for analyzing BPA in water. Samples containing BPA were analyzed, and the results were compared with the HPLC method, allowing for an evaluation of the performance and reliability of the fabricated sensors.

- The Cu,Zr-BTC/CNT/GCE sensor for BPA detection showed reliable performance with a wide linear range (2-50 μM), low detection limit (0.5 μM), high sensitivity (0.451 $\mu A \cdot \mu M^{-1} \cdot cm^{-2}$), good repeatability (RSD = 6.462%), and stability (RSD = 11.48%).

- The Fe,Ni-BTC/CNT/GCE sensor for BPA analysis enhanced charge transfer on the electrode surface. The BPA detection limit was 0.7 μM, with sensitivity of 0.334 $\mu A \cdot \mu M^{-1} \cdot cm^{-2}$, repeatability (RSD = 9.94%), and stability (RSD = 14.67%).

- The Cu,Ni-BTC/CNT/GCE sensor for BPA analysis had a detection limit of 0.5 μM and sensitivity of 0.481 $\mu A \cdot \mu M^{-1} \cdot cm^{-2}$. This electrode showed a repeatability (RSD = 13.5%) and stability (RSD = 18.55%).

Based on the results, the Cu,Zr-BTC/CNT/GCE electrode shows great potential for practical application in analyzing BPA in water due to its low detection limit, high sensitivity, and excellent repeatability and stability.

3. The Cu-BTC/GCE sensor was preliminarily studied and fabricated using the electrochemical precipitation method. The characteristic parameters and electrode material properties of Cu-BTC synthesized by this method were investigated, and the oxidation mechanism of PA on the electrode surface was predicted. The Cu-BTC/GCE sensor was applied to analyze PA in solution with the following specific results:

- The Cu-BTC/GCE sensor, fabricated using the electrochemical precipitation method, exhibited a 1.4-fold increase in charge transfer compared to the bare GCE electrode.

- The Cu-BTC/GCE sensor for PA analysis showed a low detection limit (0.077 μM) and high sensitivity (0.996 $\mu A \cdot \mu M^{-1} \cdot cm^{-2}$). Therefore, the electrochemical precipitation method is a promising method for electrode modification with potential for practical applications.

II. PERSPECTIVES

1. Improve the sensing performances of the as-develops sensors, espencially the lifetime and universality, to enable their use in practical applications.

2. More investigations in the growth mechanism of MOF film on electrode via electrochemical deposition process must be conducted to better control the morphology, structural behaviors and electrochemical behaviors of the grown films..

New Contributions of the Dissertation

1. Successfully synthesized three new composite material systems based on bimetallic MOFs combined with functionalized CNT via the solvothermal method, including:

- Cu,Zr-BTC/CNT material
- Fe,Ni-BTC/CNT material
- Cu,Ni-BTC/CNT material

2. Research results demonstrated that these materials exhibit good electrochemical activity, making them suitable for modifying GCE for rapid and selective detection of BPA.

3. Proposed a novel method for MOF film formation and successfully synthesized a Cu-BTC film directly on the GCE surface via electrochemical deposition, enabling rapid and selective detection of PA compounds in water with high sensitivity.

LIST OF THE PUBLICATIONS RELATED TO THE DISSERTATION

1. Nguyen Tien Dat, **Nguyen Ngoc Tien**, Nguyen Thi Thanh Ngan, Vu Thi Thu.

Sensing interface based on electrodeposited Cu-BTC microporous film for electrochemical detection of the painkiller paracetamol.

Analyst, 2023,148, 1777-1785

DOI: 10.1039/d3an00110e

2. **Nguyen Ngoc Tien**, Nguyen Tien Dat, Nguyen Ba Manh, Nguyen Dinh Hieu, Vu Cam Tu, Nguyen Thi Thanh Ngan, Vu Thi Thu Ha, Philippe Decorse, Benoit Piro, Vu Thi Thu.

Cu,Zr- BTC/CNT composit for electrochemical detection of endocrine disruptor BPA

J Mater Sci, 2023, 58(7), 1-15

DOI: 10.1007/s10853-023-09083-1

3. **Nguyen Ngoc Tien,** Nguyen Tien Dat, Nguyen Ba Manh, Nguyen Thi Thanh Ngan, Magdalena Osial, Marcin Pisarek, Olga Chernyayeva, Vu Thi Thu.

A simple one-pot approach to prepare composites based on bimetallic metal-organic frameworks M, Ni-BTC (M=Cu, Fe) and carbon nanotubes for electrochemical detection of bisphenol A.

J Nanopart Res (2025) 27:87

DOI: org/10.1007/s11051-025-06287-1.